Doppler effect in resonant excitation of CF_3SF_5 probed by Auger electron spectroscopy

T. Ibuki [1*], S. Itoh [1], Y. Tamenori [2], K. Okada [3], S. Nagaoka [4], Y. Morishita [5], I. H. Suzuki [5]

[1] *Kyoto University of Education, Fushimi-ku, Kyoto 612-8522, Japan*
[2] *SPring-8/Japan Synchrotron Radiation Research Institute, Mikazuki, Hyogo 679-5198, Japan*
[3] *Department of Chemistry, Hiroshima University, Higashi-Hiroshima 739-8526, Japan*
[4] *Department of Chemistry, Ehime University, Matsuyama 790-8577, Japan*
[5] *National Institute of Advanced Industrial Science and Technology, Tsukuba 305-8568, Japan*

Received

Abstract

Atomiclike Auger electron emission was observed in resonant excitation of F1*s* electron into the σ^*_{CSF} molecular orbital of CF_3SF_5. This finding means that an S−F bond forming the C−S−F linear skeleton in the ground state dissociates in the order of femto-seconds. The Auger electron emitted from the F atom showed a Doppler shift by using angle-resolved photoelectron spectroscopy. Asymmetry parameter for the leaving F atom relative to the linearly polarized electric vector was deduced to be $\beta = 1.9$ at high photon energy of 688.7 eV and a value of $\beta = 1.1$ by detuning the photon energy down to 686.8 eV. The variation of β on the exciting energies projects a profile that an axial recoil approximation effectively works for the ultrafast S−F dissociation when the $F1s^{-1}\sigma^*_{CSF}$ state is generated at high energy level on the σ^*_{CSF} potential curve but retardation effects between the F and CF_3SF_4 fragments become noticeable at low energy level where kinetic energy of the F atom gets smaller.

Keywords: *K*-shell excitation, Ultrafast dissociation, Auger electron spectroscopy, Asymmetry parameter

---

[*] Corresponding author. Tel and Fax: +81-774-27-2924, e-mail: ibuki@kyokyo-u.ac.jp

1. Introduction

Ultrafast chemical bond dissociation taking place on a time scale of a few femto-seconds was reported for the Br3*d* excitation of HBr [1] in 1986. The core excitation of HBr was recently re-examined by using the technique of two-dimensional photoelectron spectroscopy, providing more detailed features for atomic Auger decay in the two $\mathrm{Br}3d_{5/2,3/2} \rightarrow \sigma^*$ resonance transitions [2]. The ultrafast dissociations in competition with Auger electron emissions have been observed in a number of core excited diatomic molecules such as HCl [3-6], DCl [3, 4, 6], Cl_2 [3], HF [7-9], DF [8], N_2 [10] and O_2 [11-13] which decay through releasing Cl, F, N or O atom with a core hole. Similar type dissociation has been reported for triatomic H_2S [14], O_3 [15] and H_2O molecules [16] by resonant excitation of a core electron into an antibonding σ^* molecular orbital (MO). Even in polyatomic molecules of CF_4 [17] and SF_6 [18, 19], the bond fissions taking place in the low femto-second regime, termed "core-hole clock" [13], were observed and thus the phenomena seem to occur in common in chemical reactions of core excited molecules. The *K*-shell excited O_2 [12], O_3 [15], DF [8], CF_4 [17] and SF_6 [18, 19] have shown Doppler effects in angle-resolved Auger electron spectra. In these molecules O or F atom with a core hole is released through the ultrafast dissociation and then the atom ejects Auger electron giving the Doppler shift. The early research of the Auger Doppler shifts for O_2 [12] and O_3 [15] was performed at the fixed photon energies of 539.2 and 536.7 eV, respectively, which correspond to the photoabsorption maxima of $O_2 1s \rightarrow 3\sigma^*_u$ and $O_3{:}O_T 1s \rightarrow \sigma^*(7a_1)$ where O_T means the terminal O atom in ozone. The Doppler splitting and kinetic energy release of O atom were derived and discussed in the papers [12, 15]. In the work for DF [8] the Auger Doppler profile was measured by detuning excitation energies from the absorption maximum. Recent experiment for O_2 [13] was performed by employing angle-resolved electron-fragment ion coincidence spectroscopy and more detailed reaction dynamics of the *K*-shell excited O_2 were revealed. The Auger Doppler shifts for the polyatomic CF_4 [17] and SF_6 [18, 19] molecules using the third generation synchrotron radiation (SR) have been studied by detuning and by detecting electrons released into the direction parallel to the linear polarization vector of SR after exciting an F1*s* electron into a σ^* MO:

$$\mathrm{A{-}F} + h\nu \rightarrow \mathrm{A{-}F}^*(\mathrm{F}1s^{-1}\sigma^*) \rightarrow \mathrm{A} + \mathrm{F}^*(1s^1 2s^2 2p^6\,{}^2\mathrm{S}) \rightarrow \mathrm{A} + \mathrm{F}^+(1s^2 2s^2 2p^4\,{}^1\mathrm{D}) + e^-, \quad (1)$$

where A ≡ CF_3 or SF_5 and F* denotes the fluorine atom with a core hole. Photoabsorption spectrum of SF_6 gives a peak at 687.8 eV assigned to the F1$s \rightarrow a_{1g}$ transition [20], where the F* atoms formed have kinetic energies (KEs). Kitajima et al proposed an equation for analyzing the Auger Doppler profile of SF_6 [18]: Asymmetry parameter for the F* atom relative to the linear polarization of SR and that for the Auger electron relative to velocity vector of F* were deduced by a least squares curve fitting method. Kinetic energies released to the leaving F* atom and the remaining SF_5 group were also estimated by the curve fitting. The SF_6 molecule lies in a high symmetry of O_h and thus the six F atoms are able to be released as energetic F* with equal probability though one of them is excited in actuality.

Trifluoromethyl sulfur pentafluoride, CF_3SF_5, was detected in the atmosphere in 1999 and its global warning potential has been estimated to be 22000 times that of CO_2 [21]. The molecule has degrees of intramolecular freedom higher than those of SF_6 and belongs to a lower symmetry of the C_{4v} point group if we treat the CF_3 group as structureless. Total photoabsorption cross sections of CF_3SF_5 in the C, F and S *K*-shell regions were measured [22] and breakdown pathways of the *K*-shell excited CF_3SF_5 were reported [23]. The photoabsorption band peaked at 687.6 eV was assigned to the F1$s \rightarrow \sigma^*_{\mathrm{CSF}}$ transition [22] where a specific fluorine atom forming the C−S−F linear skeleton in the ground state is exclusively excited. In the present paper we report that energetic F* atom in Reaction (1) for $A \equiv CF_3SF_4$ is formed in the F1$s \rightarrow \sigma^*_{\mathrm{CSF}}$ transition followed by ionization through atomic Auger electron emission. Angle-resolved electron spectra showed typical features of a Doppler splitting. This molecule is thus the largest among the molecules in which the Auger Doppler effects have been observed. The Doppler profile was analyzed by the method proposed for SF_6 [18]. The asymmetry parameter of F* for CF_3SF_5 relative to the linear electric vector of light depends on kinetic energy release and then we elucidate dynamics for anisotropic fragmentation of the energetic F* atom.

2. Experimental

The light source was SR from a high resolution monochromator with varied-line-space plane gratings at the c-branch of the soft X-ray photochemistry beamline BL27SU of the SPring-8 facility [24]. Photon energies of 180−2800 eV were available from a Figure-8 undulator. The radiation was linearly polarized either in the plane of the electron storage ring (the first order harmonic) or in the plane perpendicular to the ring (the 0.5-th order harmonic) [25]. Photon flux of the dispersed light was monitored by measuring the drain current of the post-focusing mirror coated by gold. The experimental setup for measuring photoelectron spectra was described in detail in a previous paper [26]. In brief, an electron energy analyzer (Gammadata Scienta SES-2002) was used for the angle-resolved electron emission measurements by changing the undulator gap from the first order to the 0.5-th order harmonic without rotating the electron energy analyzer. Energy scale of the electron spectrometer was calibrated by measuring the $M_4N_{4,5}N_{4,5}$ and $M_5N_{4,5}N_{4,5}$ Auger electron emissions from xenon [27]. The resolution of the exciting SR was 150 meV and that for the energy analyzer was set to 300 meV because of weak signal intensity of the electron analyzer. The electron spectra were measured by scanning electron energy with a 0.05 eV/channel. Commercial sample of CF_3SF_5 (SynQuest Lab, stated purity >99%) was used without further purification. The base pressure of the electron energy analyzer was lower than 1×10^{-7} Pa and the sample pressure was kept at $\cong 7 \times 10^{-4}$ Pa during experiments.

3. Results and discussion

3.1 Angle-resolved photoelectron spectra

Angle-resolved electron emission spectra are shown in panel (a) of Fig. 1, being measured by tuning photon energies along the F1*s* → σ^*_{CSF} photoabsorption band depicted in panel (b) [22]. The exciting energies are indicated by numbering (1) – (5). The dotted curves in the panel (a) were accumulated by detecting electrons emitted into the direction parallel to the electric vector of SR (i.e., the first order harmonic and denoted by 0°-spectra hereafter) and the solid lines were done perpendicularly to that of SR (the 0.5-th order harmonic, 90°-spectra). The 0°- and 90°-spectra were normalized by the photon flux monitored. The 0°-spectra were plotted by shifting to upper side for clearer visibility. Peaks marked by X–G at an off-resonance excitation of 684.7 eV shifted in parallel with an increase in the exciting photon energy and were assigned to valence photoelectrons: The peak X with an ionization energy (IP) of 14.00 eV was assigned to the HOMO forming the σ_{CS} bond and the peaks A ~ G with IPs of 15.61 ~ 27.86 eV correspond to the nonbonding orbitals for electrons on the F atoms. The details are discussed elsewhere [28]. The peak labeled by H at the on-resonance excitations had no relation to the photon energy and was assigned to the atomiclike Auger electron originating from the F* atom in Reaction (1).

In a transition with $\Delta\Lambda = 0$ such as a $\Sigma_g - \Sigma_u$ excitation of diatomic molecule, fragment is ejected into the direction parallel to the electronic vector of exciting photon on the assumption of a simple axial recoil approximation [29]. In the present F1s → σ^*_{CSF} excitation with $\Delta\Lambda = 0$, the energetic F* atoms are thus preferentially released into the directions parallel to the linear electric vector of SR if the A–F* bond dissociation is highly anisotropic. The 0°-spectra show a typical Doppler shift with two wings: If the atomiclike Auger electrons are released to the directions parallel to the energetic F* atoms propagating into the electron analyzer, the electrons have sum of the Auger transition energies and KEs of the F* atoms and thus form the blue wing in the Doppler profile. The F* atoms propagating into the opposite directions have opposite sign in velocities and give the red wing. The 90°-spectra giving a single peak are produced by Auger electrons without superimposed KEs of F* since the energetic F* atoms cannot propagate into the directions perpendicular to the linear electric vector.

Figure 2 exhibits the expanded spectra for the atomiclike Auger Doppler shifts after subtraction of baseline signals originating in molecular Auger electrons. Thick dots are the experimental data and solid lines are the best fitted Doppler profile representations to be discussed in the following sections.

3.2 Cross section of resonant photoemission

Doppler effects in resonant X-Ray Raman scattering have been theoretically studied by Gel’mukhanov and coworkers who have presented the details in their publications [30-32] and claimed that the electron Doppler effect is important in nonradiative decay process. The theoretical equations proposed for the electron Doppler effects [30, 32] have been rationalized by Kitajima et al for representing an experimental cross section (σ) of the resonant Auger electron emission in the F K-shell excited SF_6 [18]:

$$\sigma(E,\omega) = \int_0^{\pi} d\theta \sin\theta \frac{\rho(\cos\theta)Q^2(\cos\theta)}{(\Delta E - kv\cos\theta)^2 + \Gamma^2}, \qquad (2)$$

where E is the Auger electron energy observed, θ is the angle between the momentum $\mathbf{k}$ of the Auger electron and the velocity vector $\mathbf{v}$ of the F* atom in the molecular frame, Γ is the lifetime width of the core excited state and $\Delta E = E - \omega_{\mathrm{cf}}$. The ω_{cf} is the peak energy of the atomiclike Auger transition. The cross section naturally depends on the exciting photon energy ω. The terms of ρ and Q^2 in the numerator of Eq. (2) are the polarization function of the molecular dissociation and the squared electronic matrix element of the Auger transition, respectively, both being dependent on the angle of θ [18]:

$$\rho(\cos\theta) = \frac{1}{3}[1 + \beta P_2(\hat{e} \bullet \hat{k})P_2(\hat{k} \bullet \hat{v})] \tag{3}$$

and

$$Q^2(\cos\theta) = 1 + \zeta P_2(\cos\theta) + \eta P_4(\cos\theta) + \tag{4}$$

where $P_2(\chi) = (3\chi^2-1)/2$ is the Legendre second order polynomial, $\hat{k} = \mathbf{k}/k$, $\hat{v} = \mathbf{v}/v$, $\hat{e}$ is the polarization vector of photon, ζ is the asymmetry parameter for the Auger electron emission relative to the velocity vector $\mathbf{v}$ of F*, and β is the asymmetry parameter of the F* fragment relative to the polarization vector. The higher order term in Eq. (4) has been assumed to be negligible [18], i.e., $\eta = 0$. The velocity v is related to the kinetic energy (ε) released to the fragments of F* and CF_3SF_4, i.e., the ε is the total kinetic energy release given by

$$\varepsilon = \frac{m_F^2 v^2}{2\mu}, \tag{5}$$

where m_F is the mass of F atom and μ is the reduced mass.

In order to numerically estimate the ω_{cf}, β, ζ and ε parameters, initial values of them were appropriately assumed for Eqs. (2) – (5) and then a set of the parameters at each photon energy was optimized by minimizing the difference between the peak areas in Fig. 2 and those calculated by Eq. (2). Here the Γ value is not known for the core excited $CF_3SF_5(F1s^{-1}\sigma^*_{CSF})$ state. For the $HF(F1s^{-1}4\sigma^*)$ Auger decay [8] it has been assumed to give a lifetime width of ≅0.2 eV on the assumption that the lifetime broadening is the same as that of 0.202 eV for the Auger transition rates of HF with two core holes which were calculated by Zähringer et al on the self-consistent-field level [33]. For the $F1s^{-1}\sigma^*$ excitation of SF_6, the $\Gamma \cong 0.1$ eV has been proposed [18].

The signal intensity of Reaction (1) for $A \equiv CF_3SF_5$ was weak since decay pathways open through decomposition of the CF_3 group and then we had to apply an experimental energy resolution of ≅0.3 eV to get good S/N ratios. In general a low energy resolution suppresses the peak heights and gives wider bands. We tentatively substitute 0.3 eV for the lifetime width of Γ. This assumed value is probably a little large and may not be close to the "pure" lifetime width of the core excited state. We do not think, however, that the value is impractical since the electron Doppler shifts in Fig. 2 are approximately equal to 0.8 eV, being large enough to be analyzed with a $\Gamma \cong 0.3$ eV in the curve fitting. The parameters of ω_{cf}, ε, β and ζ thus deduced are summarized in Table 1 and discussed in the next section. The errors given are the standard deviations.

3.3 Deduced parameters

3.3.1 ω_{cf} value and asymmetry parameter ζ for atomiclike Auger electron emission

The ω_{cf} of 656.4 ± 0.2 eV is the energy for the atomiclike Auger electron ejected from the F* fragment. The ω_{cf} value agrees with the Auger electron energies of 656.3 eV for SF_6 [18] and 656.6 eV for F atom [34], the transition of which is expressed by Reaction (1). The potential energy curves of the $F1s^{-1}\sigma^*_{\mathrm{CSF}}$ and Auger final states are expected to be parallel in the region where the Auger electron emission takes place as schematically illustrated in Fig. 3. This understanding is completely consistent with that for SF_6 [18].

Asymmetry parameter ζ relative to the velocity vector of F* lies in a constant of $\zeta = 0.31 \pm 0.08$ in the region of Ω from −0.8 to +1.1 eV, where Ω is the detuning defined as the energy difference between the exciting photon (ω) and the photoabsorption peak (E_{ab}), i.e., $\Omega = \omega - E_{\mathrm{ab}}$. The ζ value in the Auger Doppler shift of SF_6 decreases from 0.8 to 0 with an increase in Ω from −1.5 to +1.5 eV, and it has been claimed that the ζ is a function of a distance, ΔR, between the leaving F* and the remaining SF_5 group [18]: At a low excitation energy with $\Omega = -1.5$ eV the initial velocity of the F* fragment would be small and thus the A–F* state for A $\equiv SF_5$ stays on the repulsive a_{1g} potential surface having molecular character [13]. The Auger electron released in this molecular field of F* gives $\zeta = 0.8$. At a high photon energy with $\Omega = +1.5$ eV, the ΔR is large close to a dissociation limit $\Delta R \to \infty$ on the dissociative potential surface. The Auger electrons ejected through $F^*(1s^1 2s^2 2p^6\ {}^2S) \to F^+(1s^2 2s^2 2p^4\ {}^1D) + e^-$ in an atomic field are expected to be isotropic and then $\zeta = 0$ [18]. The asymmetry parameter for SF_6 in the region of $\Omega = -0.72 \sim +0.75$ eV stays constant $\zeta = 0.3 \sim 0.4$, being in agreement with the present value. The asymmetric parameter $\zeta = 0.31 \pm 0.08$ for CF_3SF_5 means that the F* atom emitting the Auger electron is not wholly atomiclike. The large CF_3SF_4 group is wrapped with negative charges on the F atoms and the directions releasing the Auger electrons are restricted by the negative charges in the present $\Omega = -0.8 \sim +1.1$ eV region.

3.3.2 Asymmetry parameter β and kinetic energy ε for F atom release*

The most interesting feature of CF_3SF_5 is the asymmetry parameter β which depends on the exciting photon energy. If we treat the A–F for A $\equiv CF_3SF_4$ as a quasi-diatomic molecule randomly oriented, the angular distribution of F* is written as the following within the axial recoil approximation [29]:

$$I(\phi) = \frac{\sigma_t}{4\pi}[1 + \frac{\beta}{2}(3\cos^2\phi - 1)], \qquad (6)$$

where σ_t is the total photoabsorption cross section over space and ϕ is the angle between the linear electric vector of light and the internuclear axis. For the excitation with $\Delta\Lambda = 0$, energetic F* atoms are released into the directions parallel ($\phi = 0°$) to the electric vector, i.e., $I(0°)$ gives a maximum. For $\Delta\Lambda = \pm1$ such as a $\Sigma - \Pi$ transition, a maximum of $I(90°)$ is observed. Using $I(0°)$ and $I(90°)$ intensities, the asymmetry parameter β is expressed by

$$\beta = \frac{2[I(0^0) - I(90^0)]}{I(0^0) + 2I(90^0)}. \qquad (7)$$

The isotropic distributions with $I(0°) = I(90°)$ give the value $\beta = 0$, a pure parallel transition with $I(90°) = 0$ gives $\beta = 2$, and $\beta = -1$ for a pure $\Delta\Lambda = \pm1$ transition with $I(0°) = 0$.

An increase in the β parameter for CF_3SF_5 with increasing the photon energy is distinctive since the β values for SF_6 have been reported to be constant $\beta \cong 1.4$ in a wide detuning region of Ω from −1.5 to +1.5 eV [18]. When the photon energy ω increases, the kinetic energy ε released to the F* and CF_3SF_4 fragments also increases (see Table 1). Here 90% of the ε are carried away by the F* atom because of the mass ratio of $m_{CF_3SF_4}/(m_{CF_3SF_4} + m_F)$. Figure 4 shows the dependence of β on the total kinetic energy ε. For the present $\Delta\Lambda = 0$ transition the β value should be $2 \geq \beta \geq 0$. The distribution of β can be approximated by a sigmoid function if we assume that the F* fragments in Reaction (1) are isotropically distributed when they have no kinetic energy, i.e., $\beta = 0$ at $\varepsilon = 0$ eV. The solid curve in the figure predicts that $\beta \leq 0.05$ at $\varepsilon \leq 1$ eV and $\beta \cong 2$ at $\varepsilon \geq 5$ eV. The value of $\beta = 1.86 \pm 0.07$ at $\varepsilon = 4.08$ eV ± 0.07 for $\omega = 688.7$ eV means from Eq. (7) that about 98% of the F* atoms are ejected into the direction parallel to the polarization vector $\hat{e}$, and for $\beta = 1.12 \pm 0.04$ at $\omega = 686.8$ eV about 20% of the F* fragments are released with the perpendicular (90°) velocity component. The former finding suggests that the F* atoms with KEs higher than ≅3.7 eV (or 4.08 eV × 0.9) are formed at high energy level on the σ^*_{CSF} potential curve and are preferentially distributed into the direction parallel to the linear electric vector of SR (see Fig. 3). The process releasing the F* atoms with KE ≅3.7 eV is probably a breakdown pathway in an atomic field on the

σ^*_{CSF} repulsive potential curve where the ΔR is large. To the contrary, the F* atoms with small KE produced at low energy level on the σ^*_{CSF} potential surface are ejected into more isotropic directions. This decay occurs in a molecular field where the ΔR is small. It is noteworthy that the asymmetry parameter at $\omega = 687.5$ eV is $\beta = 1.40 \pm 0.01$, being far from $\beta = 2$. The value of $\beta = 1.4$ implies that about 10% of the F* fragments still have the velocity component perpendicular to the C–S–F molecular axis at the σ^*_{CSF} photoabsorption maximum. We can say that the axial recoil approximation effectively works for the ultrafast F* formation at high photon energy detuned by $\Omega \cong 1$ eV, but it partly becomes ineffective in the low Ω region even at the peak-top of the σ^*_{CSF} photoabsorption band.

Depression of β value is probably due to retardation effects which are neglected in the simple axial recoil approximation given by Eq. (6). In the present large polyatomic molecule of CF_3SF_5, we think that intramolecular energy relaxation plays an important role in the retardation effects: Energy for the anisotropic S–F* dissociation in CF_3SF_5 is estimated to lie around 7.8 eV because of $\varepsilon \cong 3.7$ eV for the F* atom ejection with $\beta \cong 2$ and the bond energy of 4.06 eV for the S–F cleavage of SF_6 [35]. Excess energy in the molecule after the initial $F1s^{-1}\sigma^*_{\mathrm{CSF}}$ excitation is partly spent to produce the anisotropic F* atoms and partly would flow toward the CF_3 group with exciting molecular vibrations since the typical period of vibrations in the order of 10^{-14}–10^{-13} s is shorter than that of rotations in 10^{-12}–10^{-11} s. The C–S–F skeleton, being linear in the ground state, is thus bent to reduce the β value. The excess energy is also distributed to kinetic energies of fragments.

When we plot the ε value vs. Ω in Table 1, we get the slope of 0.64 ± 0.07 which means that about 65% of the detuning energy are shared to the total translational energies of F* and CF_3SF_5 and 35% of them are stored as the vibrational energy of the CF_3SF_5 residual. The decreasing effect in the β value becomes conspicuous at the low Ω values on the σ^*_{SCF} potential surface. The estimated threshold of $\cong 7.8$ eV for the anisotropic S–F* dissociation is considerably higher than an energy of $\cong 1$ eV distributed among vibrational degrees of freedom in the CF_3 group, being given bellow, and thus the possibility to produce anisotropic F* atoms gets low at low photon energy.

The effectiveness of the CF_3 group as an internal energy reservoir has been observed in the *K*-shell excited polyatomic molecules such as CF_3CN [36], CF_3CCH [37] and CF_3COCH_3 [38]: It has been shown that intramolecular energy flows from the initial atomic site excited toward the CF_3 group before the CF_3–R (R ≡ CN, CCH or $COCH_3$) bond fission by observing the kinetic energy distribution of the CF_3^+ ion produced. The time scale of the intramolecular energy flow is not known but the slowest limit should be less than pico-second for the bond cleavage. The internal energy of the CF_3 group is consisted of the kinetic and vibrational energies. In the present CF_3SF_5 too, excess energy flows intramolecularly from the initially excited F* atom forming the CSF skeleton toward the CF_3 group while exciting vibrational modes before the CS–F* bond dissociation.

The kinetic energies in exciting the F *K*-shell of CF_3SF_5 are lower than those of SF_6, i.e., $\varepsilon = 2.81$ eV (at $\Omega = -0.8$ eV), 3.45 (–0.1) and 3.74 (+0.6) for CF_3SF_5 are lower than $\varepsilon = 3.8$ eV (at $\Omega = -0.72$ eV), 4.3 (0.0) and 4.8 (+0.75) for SF_6 [18], respectively, by ≅1 eV at comparable Ω values. These findings imply that the energy of ≅1 eV is distributed into vibrational and translational degrees of freedom of the CF_3 group: The photoabsorption peaks for the $F1s^{-1}\sigma^*$ resonance excitations of CF_3SF_5 and SF_6 are 687.6 [22] and 687.8 eV [20], respectively, and thus the potential energy curves for the $F1s^{-1}\sigma^*$ states (see Fig. 3) should be very close. The Auger emissions through Reaction (1) are the same for both of the molecules and the potential curves for the Auger final states are expected to be parallel to those for the initial $F1s^{-1}\sigma^*$ states as discussed in the section 3.3.1. The CF_3-substitution with vibrational modes, therefore, is the most probable possibility for the kinetic energies ε less by ≅1 eV shared on the $F1s^{-1}\sigma^*_{CSF}$ potential surface of CF_3SF_5.

4. Concluding remarks

Using angle-resolved Auger electron spectroscopy, we measured an atomiclike Auger electron emission from energetic F* fragment with a core hole generated by exciting an F *K*-shell electron in the linear C–S–F skeleton of CF_3SF_5 into the repulsive σ^*_{CSF} MO. A Doppler profile was observed in the Auger electron spectra and analyzed by employing an equation proposed for the F1*s* excited SF_6. The Auger transition energy of the F* atom was 656.4 ± 0.2 eV. Auger electron emitted from the F* atom was found to have an asymmetry parameter $\zeta = 0.31 \pm 0.08$ with respect to the velocity vector of the F* fragment, which suggests that the Auger electron is emitted from the F* atom carrying a molecular-like character on the dissociative $F1s^{-1}\sigma^*_{CSF}$ potential surface. The most distinctive feature of CF_3SF_5 was an asymmetry parameter β of the leaving F* fragment relative to the electric vector of SR. The β value increased from $\beta = 1.1$ to 1.9 with an increase in kinetic energy ε of F* and CF_3SF_4 shared out at the moment of dissociative $F1s^{-1}\sigma^*_{CSF}$ excitation. The F* atoms with KE ≅3.7 eV were ejected into the direction parallel to the polarization vector of SR. The probability of F* released into the isotropic directions increased with a decrease in ε by detuning the excitation energies from 688.7 eV down to 686.8 eV along the F1*s* → σ^*_{CSF}

photoabsorption peak. A highly probable retardation effect between the leaving F* and the remaining CF_3SF_4 group was suggested to be vibrational excitation, which activates bending modes of the C–S–F skeleton and then depresses the β value in competition with the ultrafast CS–F* bond dissociation.

Acknowledgements

The authors are grateful to Prof. Kitajima of Tokyo Institute Technology for his conscientious and valuable comments on Eq. (2). We thank the members of the research team for soft X-ray photochemistry at SPring-8 for their comments. This study was carried out with the approval of the SPring-8 Program Committee (2003B0154-NSb-np) and was partly supported by a Grant-in-Aid for Scientific Research and by the Budget of Atomic Energy Research from the Ministry of the Education, Culture, Sports, Science and Technology of Japan.

References

[1] P. Morin, I. Nenner, Phys. Rev. Lett. 56 (1986) 1913.

[2] X. Feng, A.A. Wills, E. Sokell, M. Wiedenhoeft, N. Berrah, Phys. Rev. A 73 (2006) 012716.

[3] E. Kukk, H. Aksela, O.-P. Sairanen, S. Aksela, A. Kivimäki, E. Nömmiste, A. Ausmees, A. Kikas, S.J. Osborne, S. Svensson, J. Chem. Phys. 104 (1996) 4475.

[4] A. Menzel, B. Langer, J. Viefhaus, S.B. Whitfield, U. Becker, Chem. Phys. Lett. 258 (1996) 265.

[5] O. Björneholm, S. Sundin, S. Svensson, R.R.T. Marinho, A. Naves de Brito, F. Gel'mukhanov, H. Ågren, Phys. Rev. Lett. 79 (1997) 3150.

[6] E. Sokell, A.A. Wills, M. Wiedenhoeft, X. Feng, D. Rolles, N. Berrah, J. Phys. B At. Mol. Phys. 38 (2005) 1535.

[7] P. Sałek, V. Carravetta, F.Kh. Gel'mukhanov, H. Ågren, B. Schimmelpfennig, M.-N. Piancastelli, L. Sorensen, R. Feifel, I. Hjelte, M. Bässler, S. Svensson, O. Björneholm, A. Naves de Brito, Chem. Phys. Lett. 343 (2001) 332.

[8] K. Wiesner, A. Naves de Brito, S.L. Sorensen, F. Burmeister, M. Gisselbrecht, S. Svensson, O. Björneholm, Chem. Phys. Lett. 354 (2002) 382.

[9] S.E. Canton, E. Kukk, J.D. Bozek, D. Cubaynes, N. Berrah, Chem. Phys. Lett. 402 (2005) 143.

[10] M. Neeb, A. Kivimäki, B. Kempgens, H.M. Köppe, J. Feldhaus, A.M. Bradshaw, Phys. Rev. Lett. 76 (1996) 2250.

[11] C.D. Caldwell, S.J. Schaphorst, M.O. Krause, J. Jimenez-Mier, J. Electron Spectrosc. Rel. Phen. 67 (1994) 243.

[12] O. Björneholm, M. Bässler, A. Ausmees, I. Hjelte, R. Feifel, H. Wang, C. Miron, M.N. Piancastelli, S. Svensson, S.L. Sorensen, F. Gel'mukhanov, H. Ågren, Phys. Rev. Lett. 84 (2000) 2826.

[13] O. Kugeler, G. Prümper, R. Hentges, J. Viefhaus, D. Rolles, U. Becker, S. Marburger, U. Hergenhahn, Phys. Rev. Lett. 93 (2004) 033002.

[14] A. Naves de Brito, A. Naves de Brito, O. Björneholm, J. Neto, A. Machado, S. Svensson, A. Ausmees, S.J. Osborne, L.J. Sathre, H. Aksela, O.-P. Sairanen, A. Kivimaki, E. Nommisted, S. Aksela, J. Mol. Struct. (Theochem) 394 (1997) 135.

[15] L. Rosenqvist, K. Wiesner, A. Naves de Brito, M. Bässler, R. Feifel, I. Hjelte, C. Miron, H. Wang, M.N. Piancastelli, S. Svensson, O. Björneholm, S.L. Sorensen, J. Chem. Phys.

115 (2001) 3614.

[16] I. Hjelte, M.N. Piancastelli, R.F. Fink, O. Björneholm, M. Bässler, R. Feifel, A. Giertz, H. Wang, K. Wiesner, A. Ausmees, C. Miron, S.L. Sorensen, S. Svensson, Chem. Phys. Lett. 334 (2001) 151.

[17] K. Ueda, M. Kitajima, A. De Fanis, T. Furuta, H. Shindo, H. Tanaka, K. Okada, R. Feifel, S.L. Sorensen, H. Yoshida, Y. Senba, Phys. Rev. Lett. 90 (2003) 233006.

[18] M. Kitajima, K. Ueda, A. De Fanis, T. Furuta, H. Shindo, H. Tanaka, K. Okada, R. Feifel, S.L. Sorensen, F. Gel'mukhanov, A. Baev, H. Ågren, Phys. Rev. Lett. 91 (2003) 213003.

[19] G. Prümper, Y. Tamenori, A. De Fanis, U. Hergenhahn, M. Kitajima, M. Hoshino, H. Tanaka, K. Ueda, J. Phy. B Atom. Mol. Opt. Phys. 38 (2005) 1.

[20] I.G. Eustatiu, J.T. Francis, T. Tyliszczak, C.C. Turci, A.L.D. Kilcoyne, A.P. Hitchcock, Chem. Phys. 257 (2000) 235.

[21] W.T. Sturges, T.J. Wallington, M.D. Hurley, K.P. Shine, K. Sihra, A. Engel, D.E. Oram, S.A. Penkett, R. Mulvaney, C.A.M. Brenninkmeijer, Science 289 (2000) 611.

[22] T. Ibuki, Y. Shimada, S. Nagaoka, A. Fujii, M. Hino, T. Kakiuchi, K. Okada, K. Tabayashi, T. Matsudo, Y. Yamana, I.H. Suzuki, Y. Tamenori, Chem. Phys. Lett. 392 (2004) 303.

[23] T. Ibuki, Y. Shimada, R. Hashimoto, S. Nagaoka, M. Hino, K. Okada, I.H. Suzuki, Y. Morishita, Y. Tamenori, Chem. Phys. 314 (2005) 119.

[24] H. Ohashi, E. Ishiguro, Y. Tamenori, H. Okumura, A. Hiraya, H. Yoshida, Y. Senba, K. Okada, N. Saito, I.H. Suzuki, K. Ueda, T. Ibuki, S. Nagaoka, I. Koyano, T. Ishikawa, Nucl. Instrum. Meth. Phys. Res. A 467-468 (2001) 533.

[25] T. Tanaka, T. Hara, M. Oura, H. Ohashi, H. Kimura, S. Goto, Y. Suzuki, H. Kitamura, Rev. Sci. Instrum. 70 (1999) 4153.

[26] Y. Shimizu, H. Ohashi, Y. Tamenori, Y. Muramatsu, H. Yoshida, K. Okada, N. Saito, H. Tanaka, I. Koyano, S. Shin, K. Ueda, J. Electron Spectrosc. Rel. Phen. 114-116 (2001) 63.

[27] L.O. Werme, T. Bergmark, K. Siegbahn, Phys. Script. 6 (1972) 141.

[28] T. Ibuki, Y. Tamenori, K. Okada, M. Takemoto, S. Nagaoka, Y. Morishita, I.H. Suzuki, J. Electron Spectrosc. Rel. Phen. 152 (2006) 96.

[29] R.N. Zare, Mol. Photochem. 4 (1972) 1.

[30] F. Gel'mukhanov, H. Ågren, P. Salek, Phys. Rev. A 57 (1998) 2511.

[31] F. Gel'mukhanov, H. Ågren, Phys. Rep. 312 (1999) 87.

[32] H. Ågren, F. Gel'mukhanov, J. Electron Spectrosc. Rel. Phen. 110-111 (2000) 153.

[33] K. Zähringer, H.-D. Meyer, L.S. Cederbaum, Phys. Rev. A 45 (1992) 318.

[34] S. Svensson, L. Karlsson, N. Martensson, P. Baltzer, B. Wannberg, J. Electron Spectrosc. Rel. Phen. 50 (1990) C1.

[35] M.W. Chase Jr., NIST-JANAF Thermochemical Tables, 4th ed., J. Phys. Chem. Ref. Data Monograph 9 (1998) 1.

[36] T. Ibuki, K. Okada, S. Tanimoto, K. Saito, T. Gejo, J. Electron Spectrosc. Rel. Phen. 123 (2002) 323.

[37] K. Okada, S. Tanimoto, T. Ibuki, Y. Haga, T. Gejo, K. Saito, K. Ohno, Chem. Phys. 304 (2004) 273.

[38] T. Ibuki, K. Okada, M. Takahashi, S. Samori, T. Goya, Y. Senba, H. Yoshida, A. Hiraya, K. Ohno, J. Electron Spectrosc. Rel. Phen. 143 (2005) 21.

Table 1. Parameters for the Doppler profile of the atomiclike Auger electron emission.

Photon Energy, ω (eV)	Ω (eV) [a]	ω_{cf} (eV) [b]	ε (eV) [c]	β [d]	ζ [e]
686.8	−0.8	656.4 ± 0.2	2.81 ± 0.05	1.12 ± 0.04	0.25 ± 0.08
687.5	−0.1	656.4 ± 0.2	3.45 ± 0.02	1.40 ± 0.01	0.36 ± 0.06
688.2	+0.6	656.4 ± 0.2	3.74 ± 0.02	1.82 ± 0.02	0.34 ± 0.05
688.7	+1.1	656.4 ± 0.2	4.08 ± 0.07	1.86 ± 0.07	0.29 ± 0.10

[a] $\Omega = \omega - E_{ab}$ where E_{ab} = 687.6 eV is the photoabsorption peak [22].

[b] Atomiclike Auger electron energy.

[c] Kinetic energy released to F* and CF_3SF_4.

[d] Asymmetry parameter for the F* fragment relative to the polarization vector of SR.

[e] Asymmetry parameter for the Auger electron emission relative to the velocity vector **v** of F*.

Figure captions

Fig. 1. Angle-resolved electron spectra for the F1*s* → σ*$_{CSF}$ excitation. The dotted curves are the spectra observed by detecting electrons ejected into the direction parallel to the electric vector of SR and the solid lines are those detected at the perpendicular direction. Panel (b) is the F1*s* → σ*$_{CSF}$ photoabsorption cross section [22]. 1 Mb = 10^{-18} cm^2.

Fig. 2. Doppler profiles of atomiclike Auger electron emission after subtraction of baseline signals. The 0°-spectra in the left half were observed in the direction parallel to the electric vector of SR and the 90°-ones were done in the perpendicular direction. The solid lines are the best fitted results by a least-squares curve fitting.

Fig. 3. A schematic representation of atomiclike Auger electron emission in the resonant F1s → σ*$_{CSF}$ excitation of CF_3SF_5. β is the asymmetry parameter of energetic F* relative to the electric vector of SR and ζ is that for the Auger electron with respect to the velocity vector of F*.

Fig. 4. Dependence of asymmetry parameter β on the kinetic energy ε. The points with error bars are the deduced β values. The solid curve is a sigmoid function.

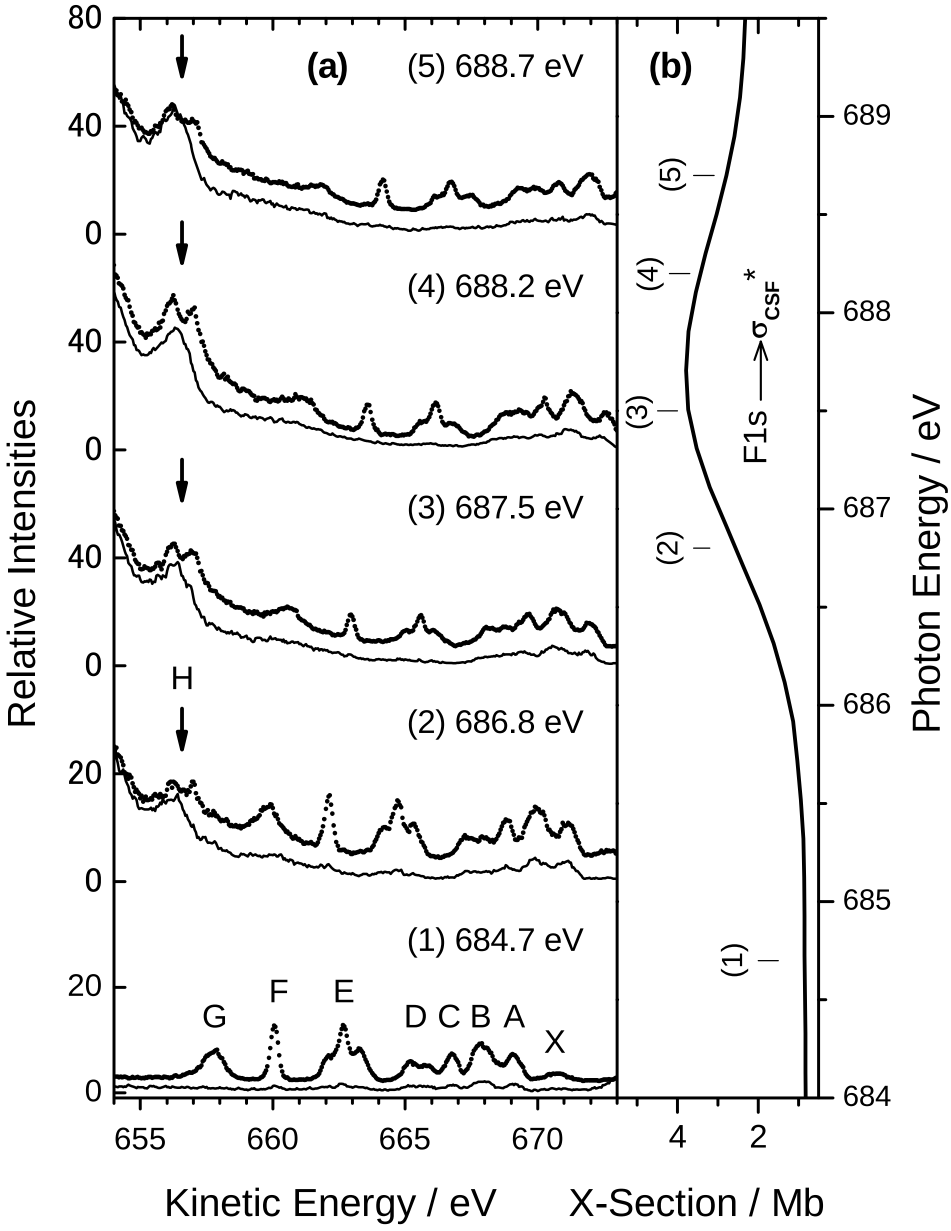

Fig. 1. T. Ibuki et al

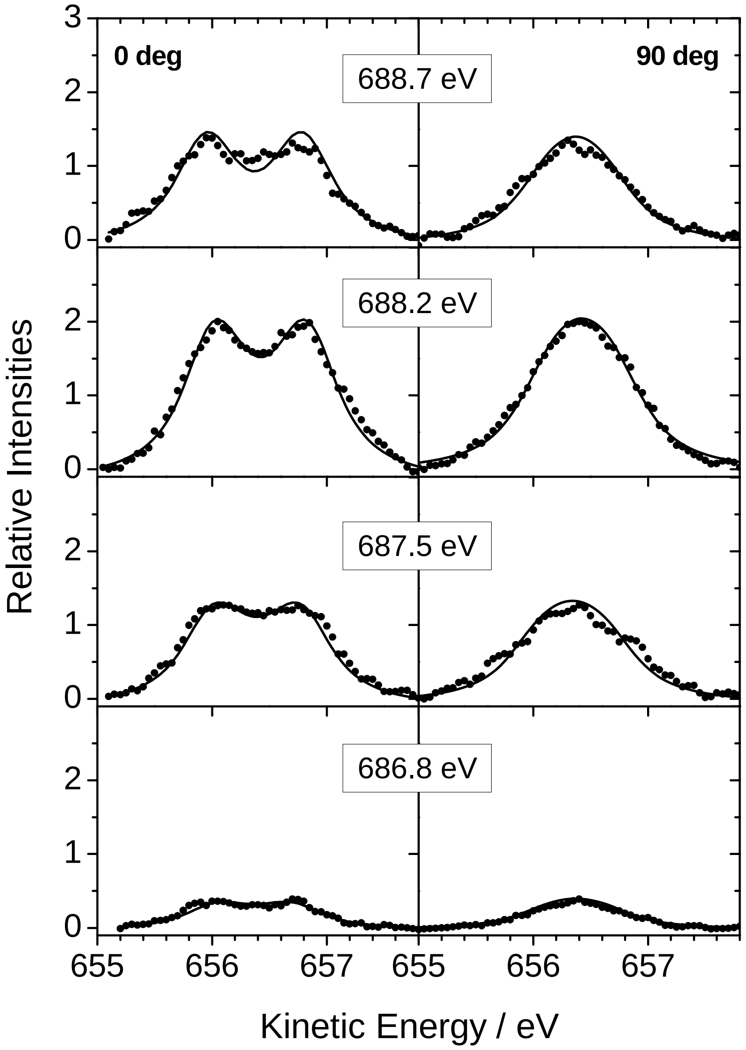

Fig. 2 T. Ibuki et al

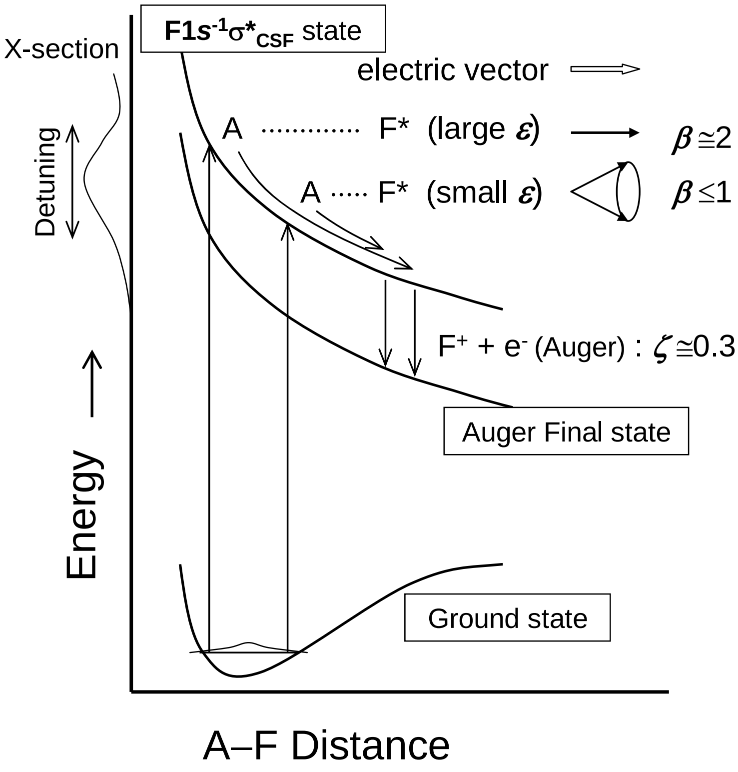

Fig. 3. T. Ibuki et al

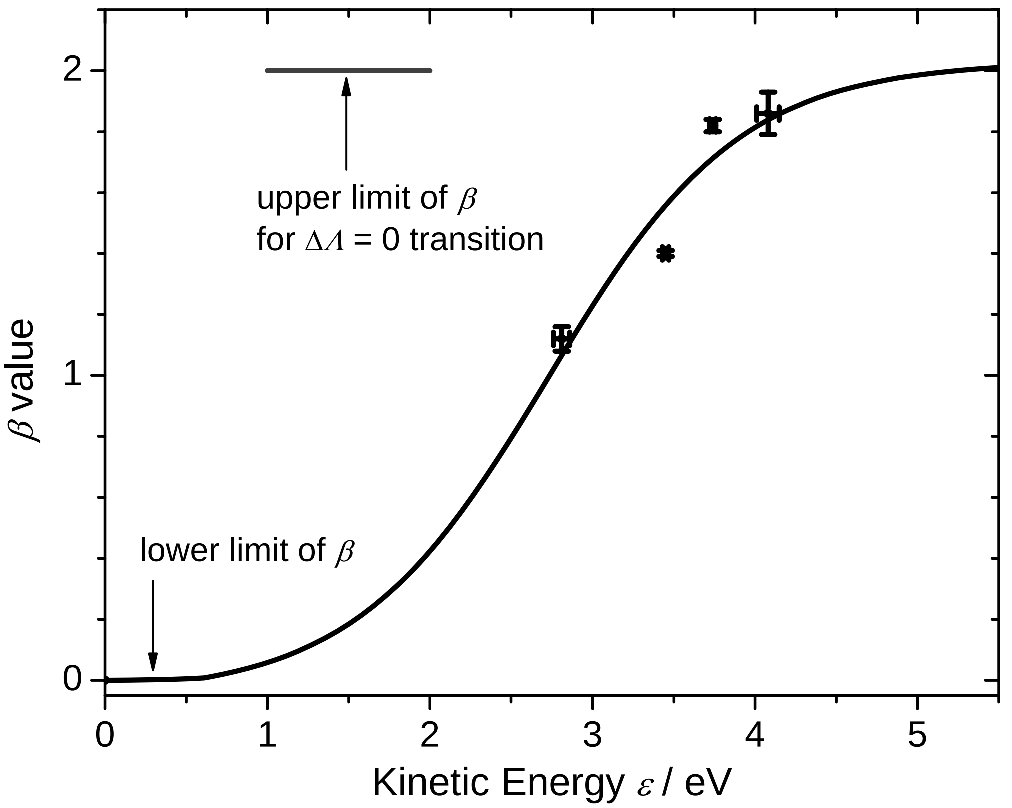

Fig. 4. T. Ibuki et al